Ferroelectrics, 367:149–162, 2008

ISSN: 0015-0193 print / 1563-5112 online
DOI: 10.1080/00150190802375227

Taylor & Francis
Taylor & Francis Group

Low-Loss Microwave Ceramics Based on Non-Stoichiometric Perovskites $Ba(Co_{1/3}Nb_{2/3})O_3$ and $Ba(Zn_{1/3}Nb_{2/3})O_3$

A. G. BELOUS,[1,*] O.V. OVCHAR,[1] O. V. KRAMARENKO,[1]
J. BEZJAK,[2] B. JANCAR,[2] D. SUVOROV,[2] AND G. ANNINO[3]

[1]V.I.Vernadskii Institute of General and Inorganic Chemistry NAS of Ukraine, 32/24 Palladin ave., Kyiv-142, 03680, Ukraine
[2]Jozef Stefan Institute, Jamova 39, 1000, Ljubljana, Slovenia
[3]Istituto per i Processi Chimico-Fisici, CNR., via G. Moruzzi 1, 56124 Pisa, Italy

The effect of both A-site and B-site non-stoichiometry on the microstructure and microwave dielectric properties of the perovskite niobates $Ba(A^{2+}_{1/3}Nb_{2/3})O_3$ (A^{2+} = Co, Zn) has been examined. Both the chemical composition of the ceramics and their sintering regimes have been shown to significantly influence the type and the amount of impurity phases which consecutively demonstrate a prevailing effect on the microwave dielectric loss. The highest magnitudes of the Qxf product have been obtained in the Co-deficient BCN (Qxf = 100 000 GHz) and Ba-deficient BZN (Qxf = 90 000 GHz) which both demonstrate noticeable amount of secondary Ba-rich phases.

Keywords Dielectrics; complex perovskites; cation ordering; quality factor

1. Introduction

Low loss dielectrics are finding numerous applications in the microwave (MW) technique. They are frequently used for the production of passive MW components like substrates for integrated circuits, dielectric-waveguides, mounting, and dielectric resonant elements including dielectric antennas or dielectric resonators [1–3]. Depending on the application field materials suitable for the MW resonant components should generally demonstrate a proper combination of dielectric parameters: high dielectric constant ($\varepsilon = 1 - 100$), high quality factor (Q) which is inverse to the dielectric loss tangent ($Q = 1/\mathrm{tg}\ \delta$) and which is often characterized by the product $Q \times \mathrm{f}$ at a frequency f ($Q \times \mathrm{f} = 10^4 - 10^5$ GHz), and close to zero temperature coefficient of resonant frequency ($\tau_\mathrm{f} = \pm 5$ ppm/K). Whereas the magnitude of dielectric constant determines the dimensions of MW component (and, accordingly, the weight and dimensions of MW apparatus) the quality factor determines the sensitivity (selectivity) of MW system, and basically, its operating frequency region

Received August 29, 2007; in final form March 11, 2008.
*Corresponding author. E-mail: belous@ionc.kar.net

[1–3]. The latter is especially relevant with the current tendency in extending working frequencies of wireless communications towards millimeter wavelength range when new cheap dielectric materials with extremely high Q – factor are required.

Until recently, the complex perovskite oxides $Ba(A^{2+}_{1/3}B^{5+}_{2/3})O_3$ (A^{2+} = Mg, Co, Zn; B^{5+} = Ta, Nb) have been generally considered as the most promising candidates to obtain the product $Q \times f \geq 100\,000$ GHz [1, 2, 4–7]. The main feature of these compounds is the presence of 1:2 ordered superstructure which comprises single layers of A^{2+} cations alternating with double layers of B^{5+} cations perpendicular to the <111> direction of the pseudocubic cell [8–10]. It is well established that B-site cation ordering in complex perovskites has a significant influence on the dielectric losses at microwave frequencies [4-6, 10-13]. This effect has been shown and proved for the tantalate perovskites $Ba(Mg_{1/3}Ta_{2/3})O_3$ (BMT) and $Ba(Zn_{1/3}Ta_{2/3})O_3$ (BZT) in which the highest magnitudes of the Q – factor have been attained [4–6, 10]. Nevertheless, the increasing costs of tantalum oxide together with the prolonged high-temperature treatment required for ensuring good properties of these materials have reoriented scientific efforts to the development of cheaper niobate-based analogues, which, moreover could be obtained in much "softer" conditions [7, 11–15]. In this sense barium cobalt niobate $Ba(Co_{1/3}Nb_{2/3})O_3$ (BCN), and barium zinc niobate $Ba(Zn_{1/3}Nb_{2/3})O_3$ (BZN) are of a special interest since they demonstrate opposite signs of their temperature coefficients τ_f [11–15]. This fact denotes a possibility to develop temperature stable materials based on the BCN-BZN solid solutions [14-16]. At the same, the reported magnitudes of the product *Qxf* scatter significantly depending on sintering conditions including sintering temperature, soaking time, cooling rate, and annealing. For instance, the authors of the Ref. 14 have got a highest product *Qxf* of about 80 000 GHz when the samples were sintered at 1400°C for 6–20 hours whereas those sintered at higher temperature (T = 1450°C) for the same time demonstrated the product *Qxf* as low as 20 000 GHz only. However, the reasons of such a discrepancy are still not clear. There are only assumptions that the variation of the Q-factor may be associated with the changes (related to the sintering conditions) in either the degree of 1:2 ordering [10–12] or the relative density (and grain growth) of a material [13, 14]. Deriving from the available data one can expect that the desired changes in the materials' structure could be intentionally induced by the slight changes in their chemical compositions. In fact, a prominent enhancement of properties has been reported fot the Mg-deficient related materials $Ba(Mg_{1/3-x}Nb_{2/3})O_3$ [17]. In contrast, the deficiency in Co did not result in any increase in the Q-factor of BCN [18]. Most recent extensive studies of non-stoichiometric BZN have found a significant influence of both Ba and Zn deficiency on the enhancement of 1:2 cation ordering, and, consequently on the product *Qxf* of sintered materials [19]. In that work the products *Qxf* of around 100 000 GHz have been obtained after annealing for 24 hours. It should be noted that the effect of annealing was different depending on the chemical composition of BZN material that resulted in a noticeable scatter in the difference between the Q-factors of as sintered and annealed samples [19], the reasons for which are not quite clear. Moreover, taking into account a strong dependence of dielectric properties of BCN, BZN, and related materials on the processing, it is still difficult to predict the upper limit to which their quality factor can be improved, for instance by annealing.

Therefore, the main goal of this work was to study the microstructure, phase composition, and microwave dielectric properties of both A-site and B-site non-stoichiometric BCN and BZN, and to find some common factors responsible for their behaviour. Another goal was to evaluate the extrinsic (related to the processing) contribution to the dielectric loss in all studied materials.

2. Experimental procedure

In this work both A-site and B-site non-stoichiometric compositions of the perovskites $Ba(A^{2+}_{1/3}Nb_{2/3})O_3$ (A^{2+}–Co, Zn) have been studied. All studied materials, therefore, can be subdivided into 4 following systems: (i) $Ba_3Co_{1+x}Nb_2O_9$; (ii) $Ba_{3+3x}CoNb_2O_9$; (iii) $Ba_3Zn_{1+x}Nb_2O_9$; (iv) $Ba_{3+3x}ZnNb_2O_9$. The ceramics were produced by the two-step conventional mixed-oxide route. At the first stage the corresponding columbites $A^{2+}_{1+x}Nb_2O_6$ (A^{2+}–Co, Zn) have been synthesized. The calcinations temperatures of the mixtures Co_3O_4-$3Nb_2O_5$ and ZnO-Nb_2O_5 have been chosen as 1150°C and 1000°C respectively. The soaking time was 4 hours. At the second stage the appropriate ratios of $BaCO_3$ and corresponding columbite were ball milled again, and calcined at 1150°C for another 4 hours. The sintering was performed in air for 8 hours at the temperatures 1350°C–1500°C. The starting reagents were extra pure MgO, ZnO, Co_3O_4 (99.95 %) and Nb_2O_5 (99.9 %). The phase composition and crystal lattice parameters of sintered ceramics were examined by means of X-ray diffraction analysis (XRD) using CuKα–radiation (Model PW 1700, Philips, Eindhoven, The Netherlands). Microstructural analysis of the ceramic samples was performed by means of scanning electron microscopy (JEOL, JSM 5800, Tokyo, Japan) using energy dispersive X-ray spectroscopy (EDX) and the LINK software package (ISIS 3000, Oxford Instruments, Bucks, UK). The dielectric characteristics of the materials ε, Q, and τ_f at frequencies around 10 GHz were examined using a cavity reflection method on the Network Analyser PNA-L Agilent N5230A. In addition, the quality factor of studied materials was examined within the frequency range of 40-70 GHz by means of Whispering Gallery Mode (WGM) technique by a millimeter wave vector analyzer model 8-350-2 (courtesy of AB millimetre, Paris, France) [20].

3. Results and discussion

3.1. The System $Ba_3Co_{1+x}Nb_2O_9$

In this system we studied compositions corresponded to $-0.15 \leq x \leq 0.03$. Both XRD and SEM analyses of sintered samples denote the formation of secondary phase only at relatively high negative x values (Co deficiency) (Figs. 1 and 2). Though, according to the XRD data the peaks of additional phase appear at $x \leq -0.1$ only, the SEM investigation revealed a slight amount of this phase even at $x = -0.07$. The peaks' positions of the impurity phase strongly resemble those of the ternary hexagonal perovskite $Ba_8ZnTa_6O_{24}$ (PDF # 45-0307) described in the Ref. 21, and hence its composition most likely corresponds to the isostructural $Ba_8CoNb_6O_{24}$ [22]. This has been confirmed also by the EDS microstructural analysis of the samples corresponding to $x = -0.15$, in which the elongated inclusions of the bright impurity phase (phase A on the Fig. 2 a) exceeded 20 μm: estimated by the EDS cation ratio was quite close to the composition $Ba_8CoNb_6O_{24}$. With increasing Co content, when $-0.07 < x \leq 0.03$ a single phase BCN is formed (Figs. 1 and 2b). Therefore, it can be stated that the BCN structure adopts a narrow homogeneity region corresponding to approximately 5% mol. Co deviation from stoichiometric amount. It is interesting to note that only stoichiometric BCN demonstrates 1:2 ordering superstructure peaks on the XRD patters (Fig. 1, curve 4). In the non-stoichiometric BCN samples these peaks were not observed.

It should be noted that the data on 1:2 ordering obtained in this work are quite inverse to those previously reported for the similar compositions [18]. The authors of the Ref. 18 observed an increase in the 1:2 ordering peaks' intensity with increasing non-stoichiometry

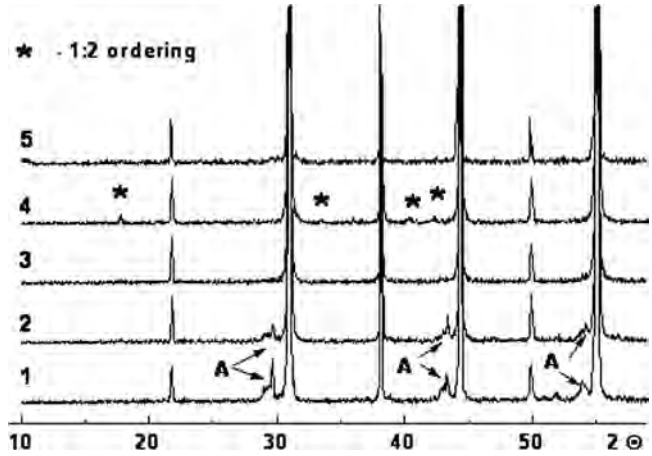

Figure 1. XRD patterns collected on the crushed powder of the samples $Ba_3Co_{1+x}Nb_2O_9$ sintered at 1470°C for 8 hours. $1-x=-0.15$; $2-x=-0.1$; $3-x=-0.07$; $4-x=0$; $5-x=0.03$; A-$Ba_8CoNb_6O_{24}$.

whereas exactly stoichiometric BCN demonstrated the poorest ordering degree. However, this difference can be attributed to the addition of 0.1 wt.% V_2O_5 to the starting powders that was used by the authors to enhance the samples' densification.

In our study an increase in the Co content was always accompanied by a monotonic increase in the density in both multiphase (MP) and single-phase regions (Fig. 3). Accordingly, the permittivity value slightly increased within studied concentration ranges from 32 to 34. In contrast to the behavior of permittivity, density, and the data of Ref. 18, the magnitude of the Q-factor passes through the maximum in the Co-deficient samples resulting in the increase in the product Qxf up to around 80 000 – 85 000 GHz within the range $-0.1 \leq x \leq -0.05$ (Fig. 4) which corresponds to the multiphase composition with no 1:2 ordering peaks observed by the XRD. At the same time, in the stoichiometric BCN the magnitude of Qxf never exceeds 55 000–60 000 GHz. The WGM characterization of sintered materials in the millimeter wavelength band (50–70 GHz) denotes a similar behavior of the Q-factor (Fig. 4). Moreover, at $x=-0.07$ the magnitude Qxf reaches values higher than 100 000 GHz that allows one to estimate the contribution of extrinsic sources (including structural distortions, secondary phases, grain boundaries and micropores) into the dielectric loss as at least 20 %. Therefore, we still have a possibility to improve the Q-factor of studied materials either by enhancing sintering process or by additional annealing. Nevertheless, from the available data it is still difficult to explain the changes observed in the Q-factor of non-stoichiometric BCN. These changes cannot be attributed neither to density nor to the degree of cation ordering which seems to be the highest in the stoichiometric BCN. Moreover, the presence of secondary phase $Ba_8CoNb_6O_{24}$-which, according to the Ref. 22 has relatively good Q ($Qxf=53\,000$ GHz)-should not result in a sharp drop of the Q-factor that is observed at negative x. Probably, the variation of the Q-factor derives from the presence of various structural defects that is indirectly denoted by the WGM results. However, this requires the further investigation into the microstructure of non-stoichiometric BCN. Another interesting result has been obtained in the Co-deficient samples with regard to their temperature coefficient of resonant frequency, which changed its sign within the range $-0.15 \leq x \leq -0.1$ (Fig. 5). This fact can be attributed to the presence of the impurity phase

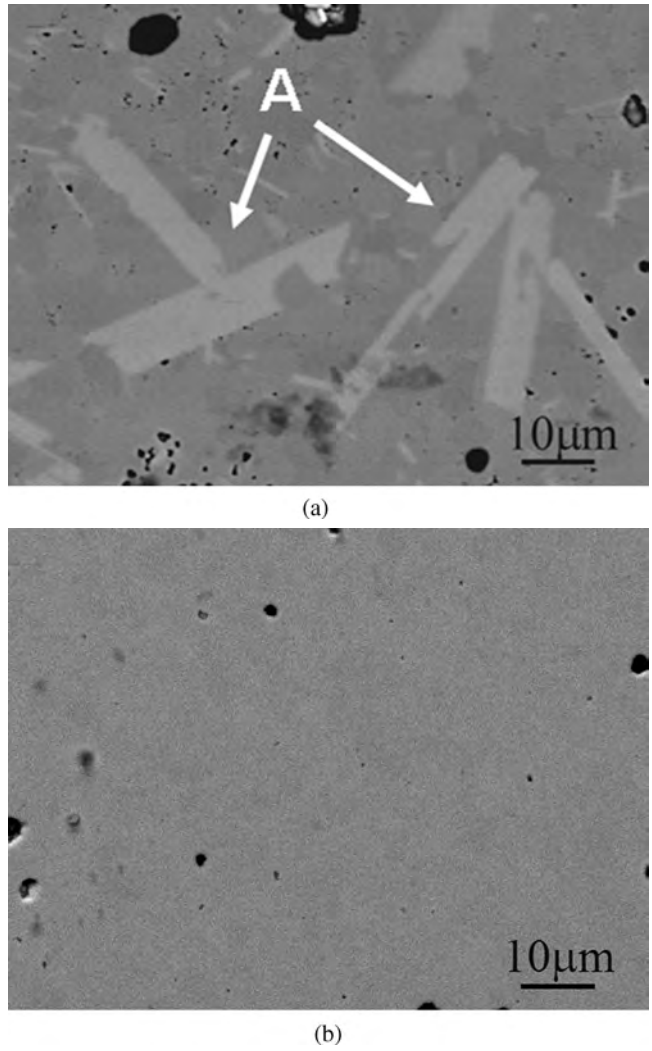

Figure 2. SEM microphotographs of the polished surface of $Ba_3Co_{1+x}Nb_2O_9$ samples sintered at 1470°C (8 h): (a) $x = -0.15$, (b) $x = 0$; A- $Ba_8CoNb_6O_{24}$.

$Ba_8CoNb_6O_{24}$ which has $\tau_f = +16$ ppm/K [22] whereas the matrix BCN exhibit τ_f with the opposite sign ($\tau_f = -7$ ppm/K). Therefore, in the Co-deficient BCN corresponding to the multiphase composition the volume temperature compensation effect appears at a certain ratio of constituting phases. As a consequence, the temperature stable dielectrics with high quality factor of around 80 000 GHz can be obtained in the BCN system simply by a proper adjustment of Co concentration.

3.2. The System $Ba_{3+3x}CoNb_2O_9$

In this system we studied compositions corresponded to $-0.1 \leq x \leq 0.01$. According to the XRD data in the case of positive x ($x \geq 0$) the single-phase materials are formed

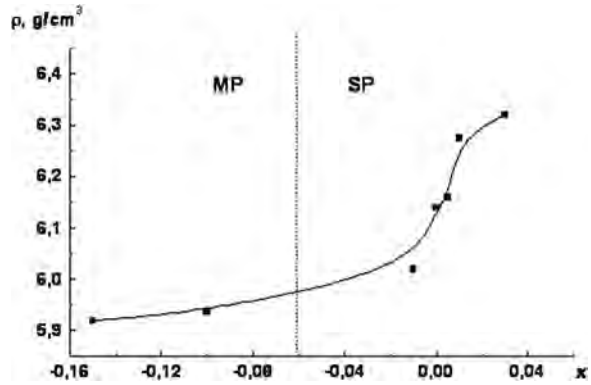

Figure 3. Relative density of the samples $Ba_3Co_{1+x}Nb_2O_9$ as a function of Co content; MP- multiphase region, SP- single-phase region.

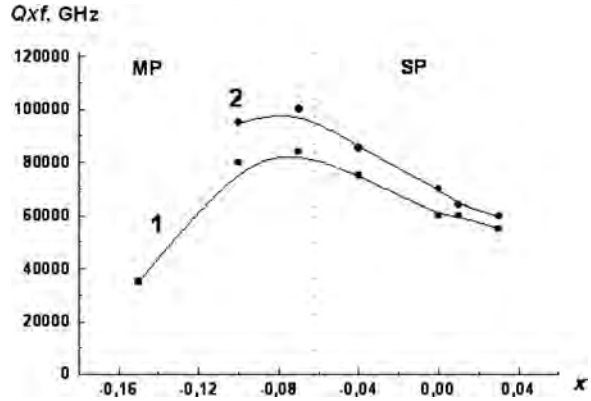

Figure 4. *Qxf* product of the samples $Ba_3Co_{1+x}Nb_2O_9$ as a function of Co content measured at the frequency 10 GHz (1), and 60 GHz (2); MP- multiphase region, SP- single-phase region.

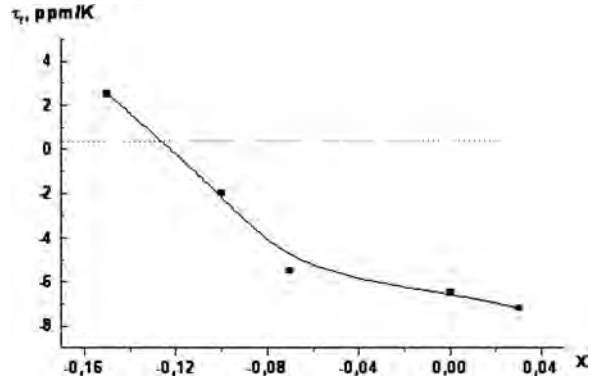

Figure 5. Temperature coefficient of resonant frequency of the samples $Ba_3Co_{1+x}Nb_2O_9$ as a function of Co content measured at the frequency 10 GHz.

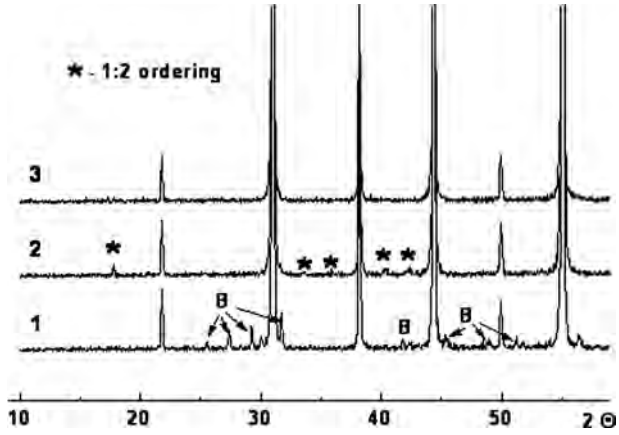

Figure 6. XRD patterns collected on the crushed powder of the samples $Ba_{3+3x}CoNb_2O_9$ sintered at 1470°C for 8 hours. $1 - x = -0.1$; $2 - x = 0$; $3 - x = 0.01$; B - $Ba_6CoNb_9O_{30}$.

(Fig. 6). When $x < 0$ a secondary phase appears with the peaks corresponding to those of $Ba_6CoNb_9O_{30}$ (PDF # 73-1879). SEM of the sintered Ba-deficient BCN revealed the presence of the Nb-rich impurity phase even at $x = -0.005$. EDS analysis of the Nb-rich phase-which is abundant in the samples with the highest Ba-deficiency ($x = -0.1$) has shown its composition to be close to the $Ba_6CoNb_9O_{30}$. This compound has been reported to have the structure of tetragonal tungsten bronze, and exhibit ferroelectric properties at room temperature [23]. It demonstrates a diffuse phase transition at 660 K, and the dielectric hysteretic at room temperature with a spontaneous polarization of $1.2(5) \times 10^{-2}$ Cm^{-2} [23]. The amount of this phase decreases in matrix with x, and completely disappears at $x = 0$ only. It should also be noted that excepting the stoichiometric BCN other sintered samples demonstrate no1:2 ordering peaks regardless of their phase assemblage (Fig. 6). Whereas the density monotonically increases with increasing amount of Ba, the permittivity of sintered materials varies only slightly within the range of $\varepsilon = 30$–33. The temperature coefficient τ_f remains practically not affected by the changes in chemical composition of the BCN. At the same time the magnitude of the Q-factor undergoes a rapid drop with a Ba-deficiency (Fig. 7). This fact is most likely associated with the effect of impurity ferroelectric phase ($Ba_6CoNb_9O_{30}$) which deteriorates dielectric properties of Ba-deficient BCN even being added to matrix in a small quantity. Surprisingly, with the further increase in the Ba content ($x > 0$) the Q-factor falls down rapidly again in the single phase materials. However, the reason for this decrease is still not cleared up.

3.3. The System $Ba_3Zn_{1+x}Nb_2O_9$

The main feature of barium zinc niobate (BZN) is that it undergoes a transition from a 1:2 ordered to disordered B-site arrangement at 1375°C [9, 12, 24]. The reduced thermal stability of the cation order requires that the samples be annealed at a temperature below 1375°C to optimize the cation ordering and the loss properties. The literature values for the Q-factor of BZN are quite varied [12–16, 19]. In contrast to other representatives of the wide family of the niobate perovskites $Ba(A^{2+}_{1/3}Nb_{2/3})O_3$, the processing of BZN is further complicated by the volatility of ZnO, which can result in the formation of impurity phases. BZN has a higher permittivity ($\varepsilon = 40$) compared with BCN ($\varepsilon = 34$) and BMN ($\varepsilon = 31$). However, it also

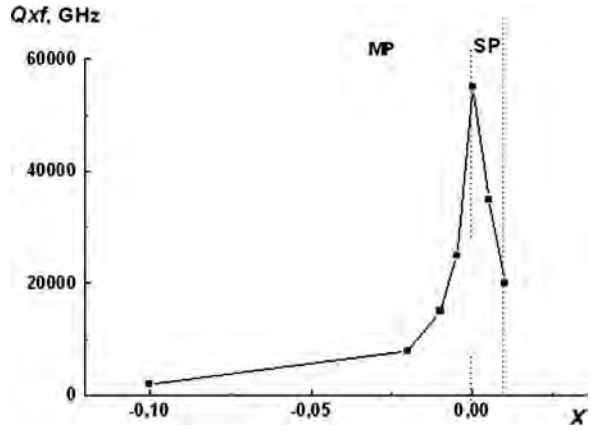

Figure 7. *Qxf* product of the samples $Ba_{3+3x}CoNb_2O_9$ as a function of Co content measured at the frequency 10 GHz; MP- multiphase region, SP- single-phase region.

has a relatively high-temperature coefficient (τ_f) of around +30 ppm/C that requires tuning, for example through the substitution of Co or Ni, prior to any practical application. The Zn non-stoichiometry induced by the partial Zn evaporation during sintering process has been previously shown to promote the 1:2 ordering [24, 25]. In the most recent investigation of BZN system the authors found the prominent effect of the chemical composition on the order/disorder temperature [19]. However, even in the non-stoichiometric BZN samples the highest product *Qxf* has been obtained only after a prolonged (50 hours) annealing at the temperature below the order/disorder transition.

According to the results obtained in our work in the studied system $Ba_3Zn_{1+x}Nb_2O_9$ ($-0.1 \leq x \leq 0.1$) the evaporation of Zn always (regardless of the chemical composition) leads to the formation of secondary Zn-free phases, which are located on the surface of the as sintered samples, and which correspond to either $Ba_5Nb_4O_{15}$ or $Ba_4Nb_2O_9$ (Figs. 8 and 9). The depth of these surface phases varies from 10 to about 100 μm depending on the sintering temperature. At the same time the bulk of the BZN ceramics represents phase assemblage

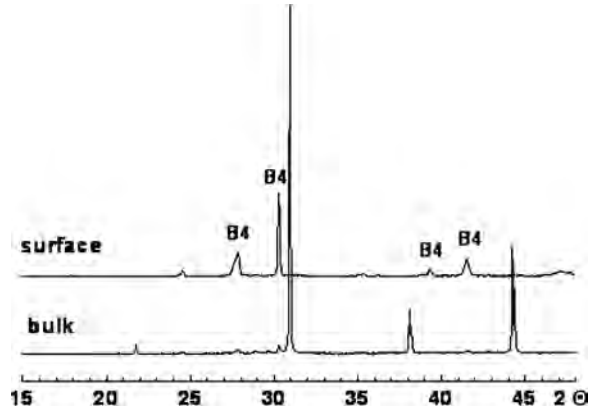

Figure 8. XRD patterns collected on the surface of as sintered at 1470°C for 8 hours samples $Ba_3Zn_{1+x}Nb_2O_9$ before (surface) and after (bulk) the polishing. B4-$Ba_4Nb_2O_9$.

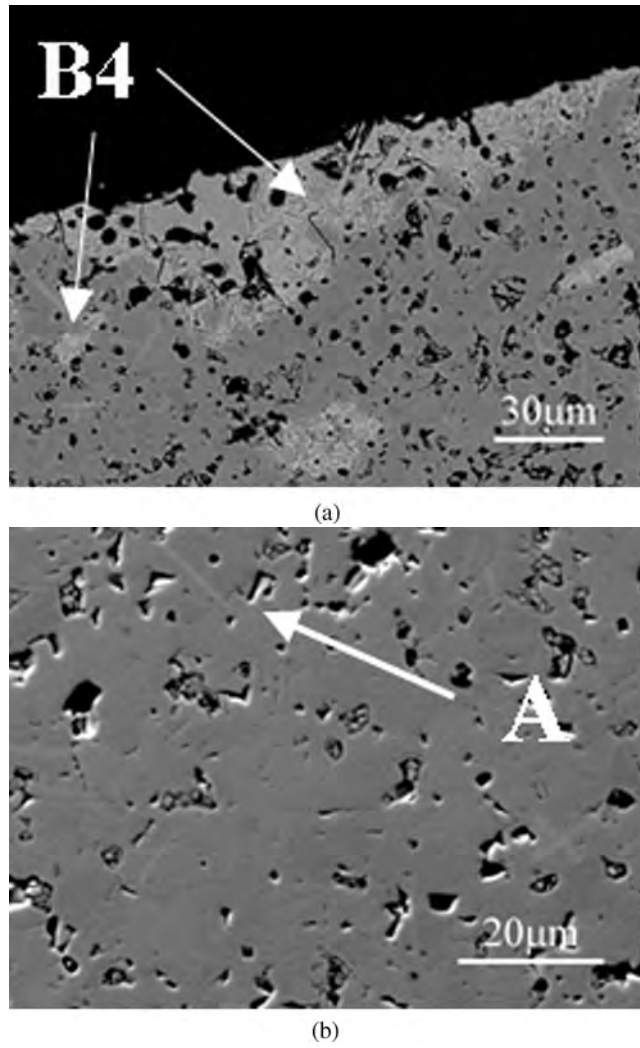

Figure 9. SEM microphotographs of the surface (a) and bulk (b) of the amples $Ba_3Zn_{1+x}Nb_2O_9$ ($x = -0.07$) as sintered at 1470°C for 8 hours. B4-$Ba_4Nb_2O_9$.

which is quite similar to that of BCN: with increasing Zn-deficiency (decreasing x) XRD data denote the formation of secondary phase isostructural to $Ba_8CoNb_6O_{24}$. According to the EDS analysis the composition of this impurity phase is close to $Ba_8ZnNb_6O_{24}$. It should be noted that—according to the XRD data—the samples sintered at 1450°C–1500°C demonstrate no 1:2 ordering peaks that is in a consistency with the literature data. With increasing x the amount of secondary phase in the bulk is reduced and is almost negligible one in the case of stoichiometric sample and at the positive x (Fig. 9b) when the ceramics is practically single phase. In the case of positive x values the sintering temperature of the materials $Ba_3Zn_{1+x}Nb_2O_9$ rapidly increases, and the ceramics corresponding to $x = 0.1$–0.4 cannot be sintered up to 1600°C demonstrating low density even after sintering at higher temperatures. Both permittivity and temperature coefficient of resonant frequency vary only slightly with the changes in chemical composition being within the ranges of

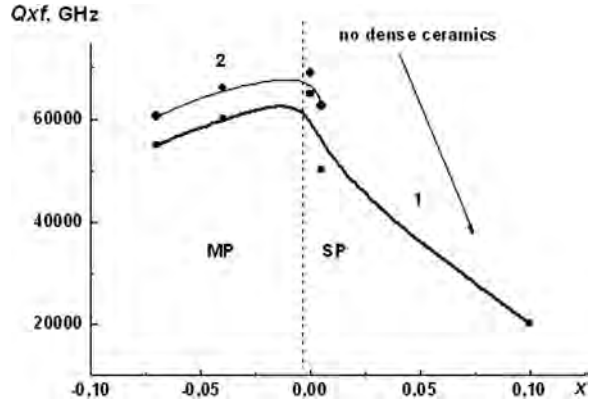

Figure 10. *Qxf* product of the samples $Ba_3Zn_{1+x}Nb_2O_9$ as a function of Zn content measured at the frequency 10 GHz (1), and 60 GHz (2); MP-multiphase region, SP-single-phase region.

$\varepsilon = 38$–41, and $\tau_f = +24 - +30$ ppm/K correspondingly. The product *Qxf* of the samples $Ba_3Zn_{1+x}Nb_2O_9$attains maximum values of around 60 000 GHz in the stoichiometric BCN whereas slightly decreases with decreasing x probably due to the increasing amount of impurity phase $Ba_8ZnNb_6O_{24}$ (Fig. 10). In the case of positive x (Zn excess) the magnitude *Qxf* falls down because of the low density of materials. Probably, additional annealing at lower temperatures could improve the quality factor of BZN samples though this requires any further studies. It should also be noted that a certain discrepancy between the data obtained in this work and those from the Ref.19 can be explained by different processing regimes since the authors of [19] muffled the samples to prevent ZnO volatilization whereas the muffling was not used in the current work.

3.4. The System $Ba_{3+3x}ZnNb_2O_9$

When investigating non-stoichiometry in the Ba-subblatice of a BZN (the system $Ba_{3+3x}ZnNb_2O_9$) x varied within the ranges $-0.1 \leq x \leq 0.005$. The samples were sintered at different temperatures within the range of $T = 1350^0C - 1450^\circ C$. When sintered at relatively low temperatures (below 1400°C) due to the poor equilibrium the materials of studied system—in addition to the matrix phase—may contain simultaneously two secondary phases including (1) the Ba-rich phase with the composition close to $Ba_8ZnNb_6O_{24}$, and (2)—Zn-containing Nb-rich analogue of ferroelectric $Ba_6CoNb_9O_{30}$ which was present in the Ba- deficient BCN. With increasing sintering temperature above 1400°C the second Nb-rich phase disappears, and the materials corresponding to $-0.02 \leq x \leq 0.005$ are single-phase (Fig. 11). However, in the case of lower x ($-0.1 \leq x \leq -0.02$) Nb-rich analogue of ferroelectric $Ba_6CoNb_9O_{30}$ was present in the matrix regardless of sintering temperature. In addition to the changes in the phase content the increasing temperature resulted in a noticeable decrease in the intensities of superstructure peaks at 17.8° on the 2 theta scale. It should be also noted that the increase in sintering temperature was always accompanied also by increasing Zn evaporation that was evident from the samples' edges: the depth of a surface edge Zn-free zone increases from 20 to above 100 μm.

Similarly to the previous system ($Ba_3Zn_{1+x}Nb_2O_9$) both permittivity and temperature coefficient of resonant frequency varied only slightly with the changes in chemical composition of the materials $Ba_{3+3x}ZnNb_2O_9$, being within the ranges of $\varepsilon = 39$–41, and

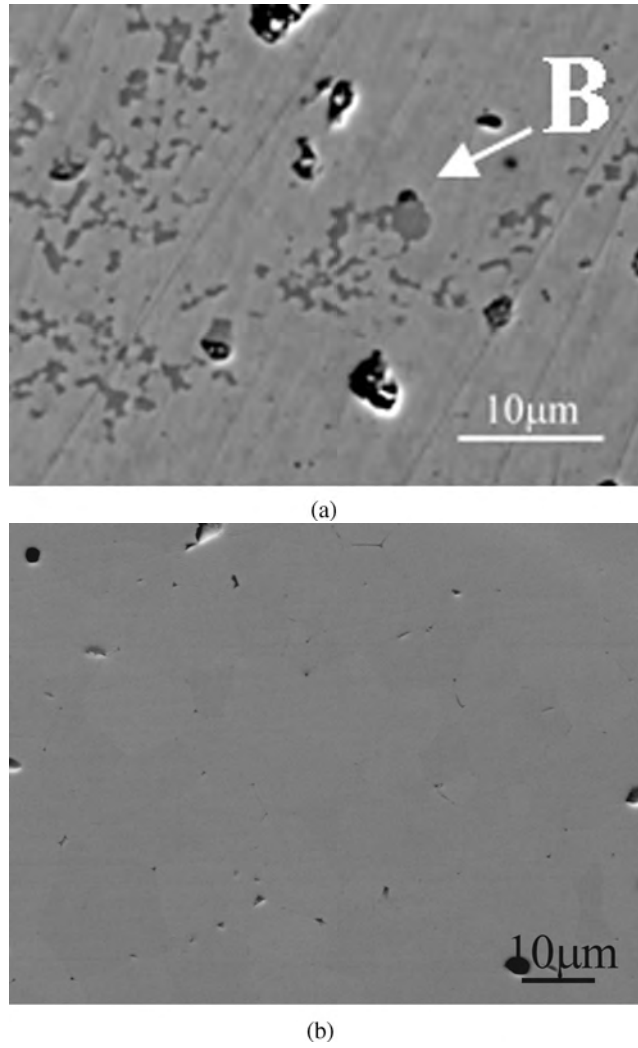

Figure 11. SEM microphotographs of the samples $Ba_{3+3x}ZnNb_2O_9$ sintered at 1370°C (a) and 1440°C (b) for 8 hours. B—$Ba_6CoNb_9O_{30}$.

$\tau_f = +24 - +30$ ppm/K correspondingly. In contrast, the product *Qxf* of studied BZN system to a large extent depends on their phase assemblage, which derives from both the chemical composition of a material and the processing regimes. When the samples are sintered at low temperatures (when they contain a large amount of impurity ferroelectric Nb-rich phase) the *Qxf* product is as low as 5000 GHz only, and starts to increase with x (Fig. 12). However, in the case of relatively slight deviation from Ba stoiciometry ($-0.02 \leq x \leq 0.005$) when the materials are sintered at higher temperatures (above 1400°C) they demonstrate product *Qxf* of about 95 000 GHz which further slightly decreases with *x* (Fig. 12). Nevertheless, in the case of higher Ba-deficiency ($-0.1 \leq x \leq -0.02$) the product *Qxf* is low due to the presence of ferroelectric Nb-rich phase. It is interesting to note that the WGM characterization of the Ba-deficient BZN samples corresponding to ($-0.02 \leq x \leq 0.005$), which has been performed at the frequencies of 40–50 GHz, did not reveal enough

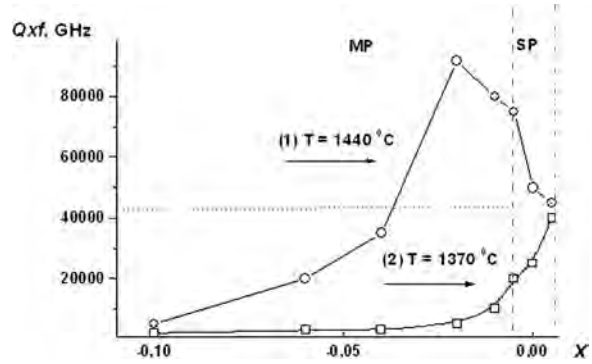

Figure 12. *Qxf* product of the samples $Ba_{3+3x}ZnNb_2O_9$ sintered at various temperatures ($T_1 = 1370^{\circ}C$, and $T_2 = 1440^{\circ}C$) as a function of Ba content; MP- multiphase region, SP- single-phase region.

strong dependence of the *Qxf* magnitude on sintering temperature as well as Ba-deficiency within studied ranges: all of the materials corresponding to $-0.02 \leq x \leq 0$ demonstrated *Qxf* magnitude within the ranges 85 000–95 000 GHz. This may denote that in the case of BZN system obtained by us *Qxf* values are already quite close to those related to the intrinsic structural sources of dielectric loss. However, taking into account the fact that the product *Qxf* of about 95 000 GHz has been obtained in the BZN materials sintered for 8 hours only, any further improvement of the *Q*-factor may be still achieved.

4. Conclusions

The microstructure, phase composition and the microwave quality factor of the perovskites $Ba(A^{2+}_{1/3}Nb_{2/3})O_3$ (A^{2+} = Co, Zn) are to a large extent effected by a deviation from stoichiometric composition. Generally, this deviation results in the formation of either Ba-rich secondary phase with the hexagonal perovskite structure and the composition close to $Ba_8A^{2+}Nb_6O_{24}$ or ferroelectric Nb-rich phase with the structure of tetragonal tungsten bronze and composition close to $Ba_6CoNb_9O_{30}$. The presence of the former phase is always accompanied by a slight reduction of the *Q*-factor whereas even low amount of the ferroelectric phase drastically degrades dielectric properties of a material. However, the obtained data denote rather weak dependence of the *Q*-factor magnitude of studied materials on the degree of cation ordering comparing to the effect of the phase assemblage and microstructure, though they do not explain an increase in the *Q* in Co-deficient BCN nad Ba-deficient BZN. The possible reasons for the observed behaviour could be related with the structural defects though this assumption requires the further extended investigation. As a consequence, the highest magnitudes of the *Qxf* product have been obtained in the Co-deficient BCN (*Qxf* = 85 000 GHz) and in Ba-deficient BZN (*Qxf* = 90 000 GHz) after sintering for 8 hours only, and without any additional annealing. The WGM characterization of studied high-*Q* materials in the millimetre wavelength band denotes a possibility in the further improvement of the *Q*-factor, especially in the non-stoichiometric BCN. Moreover the presence of hexagonal perovskite $Ba_8CoNb_6O_{24}$ in the Co-deficient BCN allows the compensation of the negative temperature coefficient of resonant frequency of the BCN matrix that can be attained without significant deterioration of its quality factor.

5. Acknowledgments

This work was partially supported by the NATO Grant under the NATO SfP project 980881: "Dielectric Resonators" of the NATO "Science for Peace" Program.

References

1. W. Wersing, Microwave ceramics for resonators and filters. Curr. Opin, *Solid State Mater. Sci*. **1**, 715–731 (1996).
2. S. J. Fiedziuszko, I. C. Hunte, T. Itoh, Y. Kobayashi, T. Nishikawa, S. N. Stitze, and K. Wakino, Dielectric Materials, Devises, and Circuits. IEEE Trans, *Microwave Theory Technol. MTT-50*, 706–720 (2002).
3. A. G. Belous, Physicochemical aspects of the development of mw dielectrics, and their use, *J. Eur. Ceram. Soc*. **21**, 2717–2722 (2001).
4. S. Kawashima, M. Nishida, I. Ueda, H. Ouchir, and S. Hayakawa, Dielectric properties of Ba(Zn,Ta)O –Ba(Zn,Nb)O ceramic. *Proc. Ferroelect. Mater. Applicat*. **1**, 293–296 (1977).
5. H. Matsumoto, H. Tamura , and K. Wakino, $Ba(Mg,Ta)O_3$-$BaSnO_3$ High-*Q* dielectric resonator, *Jpn. J. Appl. Phys*. **30**, 2347–2349 (1991).
6. S.-H. Ra and P. P. Phule, Processing and microwave dielectric properties of barium magnesium tantalate ceramics for high-quality-factor personal communication service filters. *J. Mater. Res.* **14**, 4259–4264 (1999).
7. H. Hughes, D. M. Iddles, and I. M. Reaney, Niobate-based microwave dielectrics suitable for third generation mobile phone base stations. *Appl. Phys. Letters*. **79** (18), 2952–2954 (2001).
8. F. Galasso and J. Pyle, Ordering of the compounds of the A $(B'_{0.33}Ta_{0.67})O_3$ type. *Inorg. Chem*. **2** (3), 482–484. (1963).
9. T. Takahashi, E. J. Wu, A. Van Der Ven, and G. Ceder, First-principles investigation of B-site ordering in $Ba(Mg_xTa_{1-x})O_3$ microwave dielectrics with complex perovskite structure. *Jpn. J. Appl. Phys*. **39**, 1241–1247 (2000).
10. P. K. Davis, J. Tong, and T. Negas, Effect of ordering-induced domain boundaries on low-loss $Ba(Zn_{1/3}Ta_{2/3})O_3$–$BaZrO_3$ perovskite microwave dielectrics. *J. Am. Ceram. Soc.* **80**(7), 1724–1740 (1997).
11. I. Molodetsky, and P. K. Davies, Effect of $Ba(Y_{1/2}Nb_{1/2})O_3$ and $BaZrO_3$ on the cation order and properties of $Ba(Co_{1/3}Nb_{2/3})O_3$ microwave ceramics. *J. Eur. Ceram. Soc*. **21**, 2587–2591 (2001).
12. F. Azough, C. Leach, and R. Freer, Effect of cation order on microwave dielectric properties of $Ba(Zn_{1/3}Nb_{2/3})O_3$ ceramics. *Key Eng. Mater.* **264–268**, 1153—1156 (2002).
13. S. Desu and H. M. O'Bryan, Microwave loss quality of $Ba(Zn_{1/3}Nb_{2/3})O_3$. *J. Am. Ceram. Soc.* **68**(10), 546–551 (1985).
14. C.-W. Ahn, H.-J. Jang, S. Nahm, H.-M. Park, and H.-J. Lee, Effect of microstructure on the microwave dielectric properties of $Ba(Co_{1/3}Nb_{2/3})O_3$ and (1-x)$Ba(Co_{1/3}Nb_{2/3})O_3$–x$Ba(Zn_{1/3}Nb_{2/3})O_3$ solid solutions. *J. Eur. Ceram. Soc*. **23**, 2473–2478 (2003).
15. K. Endo, K. Fujimoto, and K. Murakawa, Dielectric properties of ceramics in $Ba(Co_{1/3}Nb_{2/3})O_3$–$Ba(Zn_{1/3}Nb_{2/3})O_3$ solid solutions, *J. Am. Ceram. Soc*. **70**(9), C-215–C-218 (1987).
16. F. Azough, C. Leach, and R. Freer, Effect of V_2O_5 on the sintering behaviour, cation order and properties of $Ba_3Co_{0.7}Zn_{0.3}Nb_2O_9$ ceramics. *J. Eur. Ceram. Soc*. **25**, 2839–2842 (2005).
17. J. H. Paik, I. T. Kim, J. D. Byun, H. M. Kim, and J. Lee, The effect of Mg deficiency on the microwave dielectric properties of $Ba(Mg_{1/3}Nb_{2/3})O_3$ ceramics. *J. Mat. Sci. Letters*. **17**, 1777–1780 (1998).
18. F. Azough, C. Leach, and R. Freer, Effect of nonstoichiometry on the structure and microwave dielectric properties of $Ba(Co_{1/3}Nb_{2/3})O_3$ ceramics. *J. Eur. Ceram. Soc*. **26**(14), 2877–2884 (2006).
19. H. Wu and P. K. Davies, Influence of non-stoichiometry on the structure and properties of $Ba(Zn_{1/3}Nb_{2/3})O_3$ microwave dielectrics: II. compositional variations in pure BZN. *J. Am. Ceram. Soc*. **89**(7), 2239–2249 (2006).

20. G. Annino, D. Bertolini, M. Cassettari, M. Fittipaldi, I. Longo, and M. Martinelli, Dielectric properties of materials using whispering gallery dielectric resonators: Experiments and perspectives of ultra-wideband characterization. *J. Chem. Phys*. **112**, 2308–2314 (2000).
21. A. M. Abakumov, G. Van Tendeloo, A. A. Scheglov, R. V. Shpanchenko, and E. V. Antipov, The crystal structure of $Ba_8Ta_6NiO_{24}$: Cation ordering in hexagonal perovskites. *J. Solid State Chem*. **125**, 102–107 (1996).
22. P. M. Mallinson, M. M. Allix, J. B. Claridge, R. M. Ibberson, D. M. Iddles, T. Price, and M. J. Rosseinsky, $Ba_8CoNb_6O_{24}$: a d^0 dielectric oxide host containing ordered d^7 cation layers 1.88 nm apart, *Angew. Chem. Int. Ed. Engl*. **44**(47), 7733–1136 (2005).
23. M. C. Foster, G. R. Brown, R. M. Nielson, and S. C. Abrahams, $Ba_6CoNb_9O_{30}$ and $Ba_6FeNb_9O_{30}$: Two new tungsten-bronze-type-like ferroelectrics. *J. Appl. Cryst*. **30**, 495–501 (1997).
24. K. S. Hong, I.-T. Kim, and C.-D. Kim, Order–disorder phase formation in complex perovskite compounds $Ba(Ni_{1/3}Nb_{2/3})O_3$ and $Ba(Zn_{1/3}Nb_{2/3})O_3$. *J. Am. Ceram. Soc*. **79**(12), 3218–3224 (1996).
25. P. K. Davies, A. Borisevich, and M. Thirumal, Communicating with wireless perovskites: cation order and zinc volatilization. *J. Europ. Ceram. Soc*. **23**, 2461–2466 (2003).